MULTICOMPONENT GAS ADSORPTION ON MSC5A BY CHROMATOGRAHIC METHOD AND STOP & GO SIMULATION

Kazuyuki CHIHARA[1*], *Yuki TERAMURA*[1], *Hidenori NAKAMURA*[1] *and Yosuke KANEKO*[1]
Meiji University
Higashi-mita, Tama-ku, Kawasaki, Japan

Abstract

Perturbation chromatography with multi component gas carrier and non-equilibrium thermodynamics liner law was applied for discussion of the interference effect and the displacement effect on mass transfer in multi component gas adsorption. Moment analysis method and stop & go simulation method were utilized to obtain each mass transfer parameters of adsorbate gases. Dependency of micropore diffusion on amount adsorbed and correlation of micropore diffusion with chemical potential driving force for microporous adsorbent were confirmed. Cross effect in micropore diffusion was found.

Keywords

chromatograph, stop & go simulation, multi component gas

1. Introduction

The combination of chromatographic method and moment analysis of the response peaks is one of the useful techniques to study adsorption equilibrium and adsorption rate (Chihara et al. 1978). Perturbation chromatography with the mixed multi component adsorbate gas carrier (two adsorbates) has been applied to several studies on adsorption (Ruthven and Kumar 1979, Kumar et al. 1982). In this work, perturbation chromatography with multi component gas carrier (two adsorbates with inert gas) and non-equilibrium thermodynamics liner law was applied for discussion of the interference effect and the displacement effect (those are cross effects) on mass transfer in multi component gas adsorption as previous study (Chihara et al. 2005) for different gas mixture (He, N_2, CH_4). Moment analysis method and stop & go simulation method were utilized to obtain each mass transfer parameters of adsorbate gases. Dependency of micropore diffusion on amount adsorbed and correlation of micropore diffusion with chemical potential driving force for microporous adsorbent were discussed. Also, cross effect were discussed. Ruthven already pointed the dependency of micropore diffusivity on amount adsorbed in single component adsorption (Ruthven 1984). Tondeur et al gave general background on multi component perturbation chromatography for the first moment only (Tondeur 1996).

2. Experimental Method

2.1. Experimental Procedure and Conditions

The experimental apparatus was shown in figure1. The apparatus was similar to a conventional gas chromatograph. Adsorbent particles (molecular sieving carbon 5A, 20/30 mesh, Japan Enviro Chemical Ltd.,) were packed in a column (100cm x 3mm i.d.). Carrier gas was a mixture of two or three components among He, CH_4, CO_2. Perturbation pulse was introduced into the carrier gas stream.

Introduction of pulses was performed by 6-way valve. The pulse size was 1cc, which meant injection period was 1.4 sec. Then pulse response was detected by TCD cell. Output signal of TCD was transmitted to a personal computer through RS232C. This signal was also transmitted to the personal computer. Simulated chromatogram by a personal computer can be overlapped on experimental chromatogram shown in the monitor screen. Further, moment of pulse response, which is shown in the monitor screen, can be automatically calculated by the personal computer. The first absolute moment and the second central moment were evaluated from the effluent peak $C_e(t)$ as follows:

$$\mu_1 = \int_0^\infty C_e(t)tdt \Big/ \int_0^\infty C_e(t)dt \qquad (1)$$

$$\mu_2{}' = \int_0^\infty C_e(t)(t-\mu_1)^2 dt \Big/ \int_0^\infty C_e(t)dt \qquad (2)$$

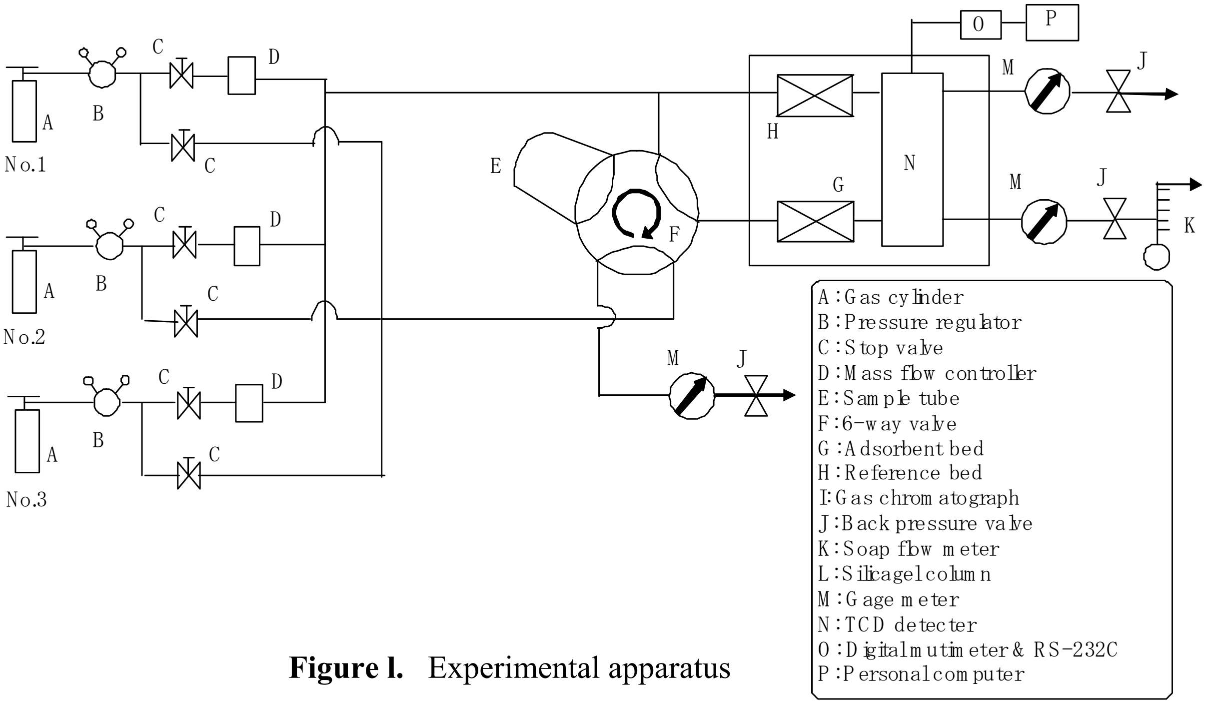

Figure l. Experimental apparatus

Moment Analysis

Basic equations are in ref. (Kumar et al. 1982)

The resultant moment equations of the impulse response are

$$\mu_1 = \frac{z}{u}\left\{1 + \frac{(1-\varepsilon)\rho_p(1-y)K^*}{\varepsilon}\right\} \qquad (3)$$

$$\mu_2 = \frac{2z}{u}\left[Ez\left\{\frac{1+(1-\varepsilon)\rho_p K^*}{\varepsilon u}\right\}^2 + \frac{(1-\varepsilon)\rho_p(1-y)K^*}{\varepsilon Ksav}\right] = \frac{2z}{u}(\delta_d + \delta_f + \delta_a + \delta_i) \qquad (4)$$

where μ_1=first absolute moment of the chromatographic peak[s] μ_2=second central moment[s^2].

$$\delta_d = \frac{Ez}{u^2}\left\{1 + \frac{(1-\varepsilon)\rho_p(1-y)K^*}{\varepsilon}\right\}^2 \qquad (5)$$

$$\delta_f = \frac{1-\varepsilon}{\varepsilon}\frac{R}{3k_f}\rho_p{}^2(1-y)K^{*2} \qquad (6)$$

$$\delta_a = \frac{1-\varepsilon}{\varepsilon}\frac{R^2}{15D_a}\rho_p{}^2(1-y)K*^2 \quad (7) \qquad\qquad \delta_i = \frac{1-\varepsilon}{\varepsilon}\frac{\rho_p(1-y)K*}{15D}\bar{a}^2\exp(\sigma^2) \quad (8)$$

where $K*$=apparent adsorption equilibrium constant, Ez=axial dispersion coefficient based on void spaces in the bed, k_f=external mass transfer coefficient, D_a=diffusivity in macropores and D_i=diffusivity in micropores based on amount adsorbed gradient driving force. The arithmetic average radius $\bar{a}$ is 8.2 μm (Chihara, Suzuki and Kawazoe 1978).

Equation(3) was used along with the experimental μ_1 to obtain the adsorption constant $K*$. Equation(4) to (8) were used along with the experimental μ_2' to obtain the diffusivity in micropores D.

Stop & Go Simulation

Numerical solution for multi component chromatogram in time domain could be obtained by appropriate model equations with experimental conditions. This simulated chromatogram can be compared with experimental chromatogram to determine the equilibrium and the adsorption kinetic parameters. Here Markham-Benton equation as for adsorption equilibrium and linear driving force (LDF) approximation as for adsorption kinetics were adapted for numerical calculation, which was based on stop & go method (Chihara et al. 1986, Chihara and Kondo 1986). In particular, LDF model of adsorption kinetics was based on non-equilibrium thermodynamics.

For binary adsorbates, adsorption rate equations are

$$\gamma\frac{\partial q_1}{\partial t} = Ksav_{1,1}(q_1*-q_1)+Ksav_{1,2}(q_2*-q_2) \quad (9) \qquad \gamma\frac{\partial q_2}{\partial t} = Ksav_{2,1}(q_1*-q_1)+Ksav_{2,2}(q_2*-q_2) \quad (10)$$

where $Ksav$= Overall mass transfer coefficients.

Overall mass transfer coefficients ($Ksav$) for LDF model were determined. Then, micropore diffusivities were obtained by subtracting other mass transfer effects from overall resistance ($\gamma/Ksav$). Thus obtained micropore diffusivities were correlated with chemical potential driving force by consideration of Fick's diffusion equation, non-equilibrium thermodynamics and extended Langmuir equation (Karger and Bulows 1975).

$$\frac{D_{11}}{a^2} = \frac{D_1'}{a^2}\frac{\partial\ln p_1}{\partial\ln q_1} = \frac{D_1'}{a^2}\frac{1-\theta_2}{1-\theta_1-\theta_2} \quad (11) \qquad \frac{D_{12}}{a^2} = \frac{D_1'}{a^2}\frac{q_1}{q_2}\frac{\partial\ln p_1}{\partial\ln q_2} = \frac{D_1'}{a^2}\frac{\theta_1}{1-\theta_1-\theta_2} \quad (12)$$

$$\frac{D_{21}}{a^2} = \frac{D_2'}{a^2}\frac{q_2}{q_1}\frac{\partial\ln p_2}{\partial\ln q_1} = \frac{D_2'}{a^2}\frac{\theta_2}{1-\theta_1-\theta_2} \quad (13) \qquad \frac{D_{22}}{a^2} = \frac{D_2'}{a^2}\frac{\partial\ln p_2}{\partial\ln q_2} = \frac{D_2'}{a^2}\frac{1-\theta_1}{1-\theta_1-\theta_2} \quad (14)$$

For instance, $Ksav$ is related to D in single adsorbate case as

$$\frac{1}{Ksav} = \frac{a^2}{15D} + K*\left(\frac{R}{3k_f} + \frac{R^2}{15\varepsilon D_a}\right) \quad (15)$$

For binary case, when using Equation (15), apparent $K*$ could be determined by appropriate slope of adsorption isothermal plane at perturbation point.

3. Result And Discussion

3.1. Single Adsorbate Carrier Mixed with He and The Same Adosorbate Pulse

Figure 2. shows an example of comparison of experimental chromatogram with simulated chromatogram for MSC5A to obtain *Ksav* for LDF model. Experimental conditions were 313 K, column pressure 5 atm, flow rate 25 cm/sec and He+CH_4 mixed gas carrier with CH_4 pulse. Here CH_4 concentration in the carrier gas was changed 10, 30, 50, 70 and 90 %.

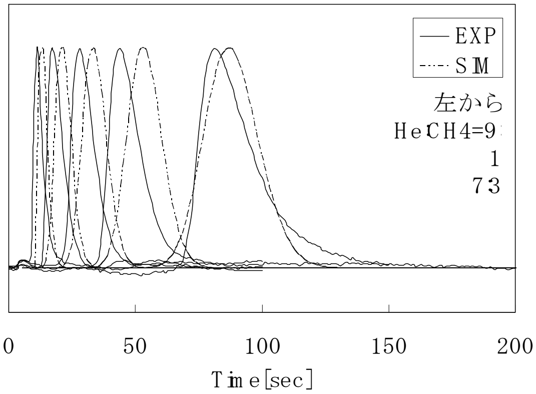

Figure 2. Comparison of experimental peaks with simulation

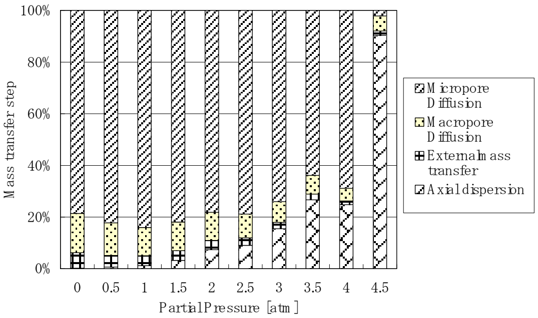

Figure 3. Mass transfer steps of CH_4 on to MSC5A

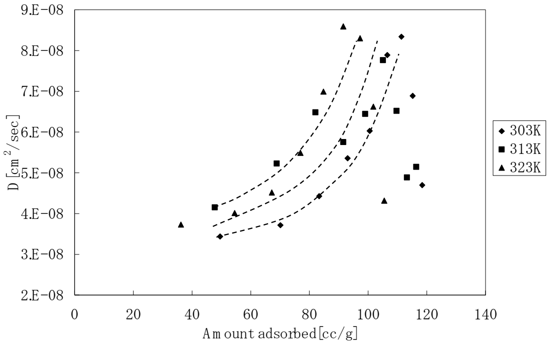

Figure 4. Dependency of micropore diffusivity coefficient on the amount adsorbed

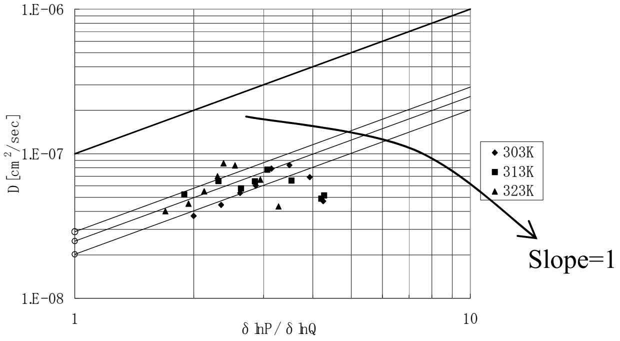

Figure 5. Correlation based on chemical potential driving force

Figure 3. shows contribution of axial dispersion, external mass transfer, macropore diffusion and micropoore diffusion in case of CH_4 for MSC5A at 323 K. This figure illustrated that mass transfer is controlled by micropore diffusion.

Figure 4. shows the dependency of micropore diffusivity coefficient of CO_2 with amount adsorbed at 303, 313 and 323 K for MSC5A.

Figure 5. shows the correlation of micropore diffusivity of CO_2 with chemical potential driving force at 303, 313 and 323 K for MSC5A. Proportional relation was obtained, which means that micropore diffusion is based on chemical potential driving force.

3.2. Binary Adsorbate Carrier Mixed with He and Adsobate Pulse

Figure 6-(a) and (b) show experimental and simulation results in an example case of binary adsorbate carrier mixed with He and an adsorbate pulse for MSC5A. Experimental conditions were 323 K, column pressure 5 atm, flow rate 25 cm/sec and He(60%)+CO_2(10%)+CH_4(30%) mixed gas carrier with CO_2 pulse. Figure6-(a) is the comparison between experimental and simulated TCD peaks. Two simulated TCD peaks are those for accounted and not accounted for cross effect. Figure6-(b) is simulated peaks of each gas component and total peak. The total peak is assumed to be the sum of adsorbate peaks except He and assumed to be as simulated TCD peak, which was found to be conincident with experiment as in Figure6-(a).

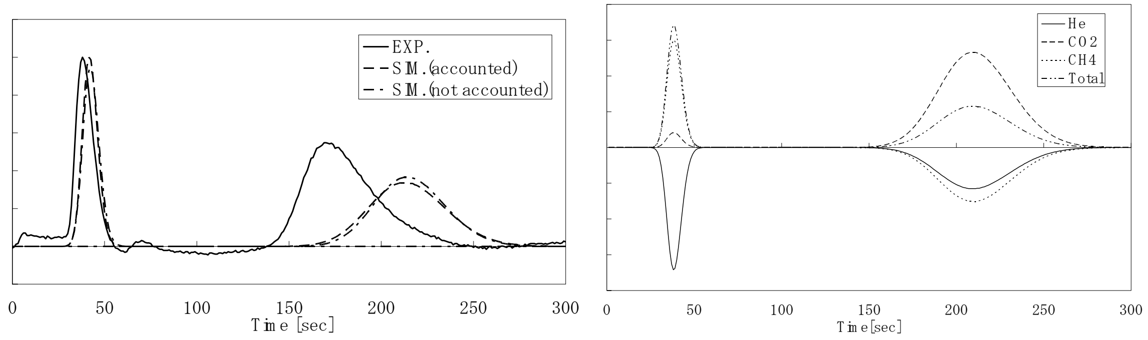

(a) (b)

Figure6. Comparison between experimental chromatogram and simulated one (a), Simulation of pulse response of each component (b)

Simulated chromatogram for CO_2 and CH_4 mixture may be regarded as co-diffusion or competitive adsorption for 1st peak and as counter-diffusion or displacement adsorption for 2nd peak.

1st peak shows good agreement between experimental peak and simulated peak. But 2nd peak is not. So it is hard to judge the propriety.

The sum and product of two peaks' retention times can be related with isothems (Glover 1983).

$$
\begin{aligned}
&(1-y_1^*)\left(\frac{\partial g_1}{\partial y_1}\right)^* + (1-y_2^*)\left(\frac{\partial g_2}{\partial y_2}\right)^* - y_1^*\left(\frac{\partial g_2}{\partial y_1}\right)^* \\
&\qquad - y_2^*\left(\frac{\partial g_1}{\partial y_2}\right)^* = \frac{N}{M_s}(t_{ra}+t_{rb}) \\
&\left(\frac{\partial g_1}{\partial y_1}\right)^*\left(\frac{\partial g_2}{\partial y_2}\right)^* - \left(\frac{\partial g_1}{\partial y_2}\right)^*\left(\frac{\partial g_2}{\partial y_1}\right)^* \\
&\qquad = \left(\frac{N}{M_s}\right)^2 \frac{t_{ra}t_{rb}}{(1-y_1^*-y_2^*)}
\end{aligned}
\tag{16}
$$

In this study, eq. (16) is rewrited as follows, assuming extended Langmuir isotherm.

$$
\begin{aligned}
&\frac{p_0}{(1+K_1p_1+K_2p_2)^2}\{(1-y_1)q_{\infty1}K_1(1+K_2p_2) \\
&\qquad +(1-y_2)q_{\infty2}K_2(1+K_1p_1)\} \\
&+\frac{p_0K_1K_2}{(1+K_1p_1+K_2p_2)^2}(y_1q_{\infty2}p_2+y_2q_{\infty1}p_1) \\
&=\frac{V_r}{M_s}(t_{ra}+t_{rb}) \\
&\frac{p_0^2q_{\infty1}q_{\infty2}K_1K_2}{(1+K_1p_1+K_2p_2)^2}\{(1+K_1p_1)(1+K_2p_2) \\
&\qquad -K_1p_1K_2p_2\} \\
&=\left(\frac{N}{M_s}\right)^2\frac{t_{ra}t_{rb}}{(1-y_1-y_2)}
\end{aligned}
\tag{17}
$$

Where p_0= column pressure (5 atm), K = Langmuir constant, q_∞= saturation amount adsorbed, t_r = retention time, V_r = volume flow rate at 1 atm, M_s = amount of MSC5A in column.
This relation could be used to check experimental and simulated results with assumed isotherm as table 1.

Table 1. The sum and product of two peaks retention times

	Sum [sec]	Product[sec^2]
Exp.	212	6747
Sim.	257	9030
From isothem	242	6664

Sum value of calculation is close to simulation. But, product is close to experiment.

Figure 7. shows Ksav obtained by Eq.(11)~(15) neglecting macro effect for binary adsobates system, corresponding to Figure 6. It was found that *Ksav* obtaind by consideration of chemical potential driving force with cross effect was well applied to get good simulation results for multicomponent pulse response though some discrepancies were founded.

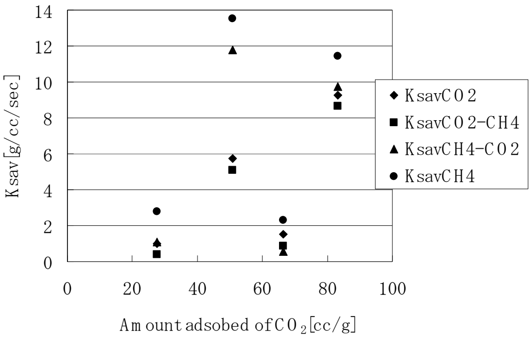

Figure 7. Comparison of *Ksav* of single adsorbate, and *Ksav* of binary adsorbate[He+ CH_4- CO_2]

4. Conclusion

This time, we cannot get good agreements between experimental chromatogram and simulated chromatogram, based on the modeling of Stop & Go method, in case of peturbation chromatography with mixed adsorbate gas carrier. And micropore diffusivities obtained were interpreted by chemical potential driving force consideration based on non-equilibrium thermodynamics law. Some possibilitty was shown for cross effect of micropore diffusion in multicomponent adsorption.

5. References

Chihara K. et al; "Simulation of Pressure Swing Adsorption for Air Separation" Proc. 7th Int. zeolite Conf.,563(1986)

Chihara K. and Kondo A.; "Simulation of Pressure Swing Adsorption –Three Gas Components and Three Adsorption Columns-" 2nd FOA, 165 (1986)

Chihara, K., Suzuki M. and Kawazoe K.; "Adsorption Rate on Molecular Sieving Carbon by Chromatography" AIChE J., 24, 237 (1978)

Chihara K. et al; "Study of Multicomponent Gas Adsorption into MSC5A by Chromatograph" Adsorption, 11, 249-253(2005)

Glober C. J. and Lau W. R.; "Determination of Multicomponent Sorption Equilibria Using Perturbation Gas Chromatograpy" AIChE J., 29, 73-79 (1983).

Karger J. and Bulows M.; Chem. Eng. Sci., 30, 893(1975)

Kumar R., Duncan R.C. and Ruthven D.M.; "A Chromatographic Study of Diffusion of Single Components and Binary Mixtures of Gases in 4A and 5A Zeolites" Can.J.Chem.Eng., 57, 342 (1982)

Tondeur D., Kabir H., Luo L., and Granger J.; "Multicomponent adsorption equilibria from impulse response chromatography" Chem. Eng. Science, 51(N15) 3781-3799 (1996)

Ruthven D.M,; "Principle of Adsorption and Adsorption Process" Wiley, 146 (1984)

Ruthven D.M. and Kumar R.; "A Chromatographic Study of the Diffusion of N_2, CH_4 and Binary CH_4-N_2 Mixtures in 4A Molecular Sieve" Can.J.Chem.Eng., 57, 342 (1979)